Journal of Experimental Botany, Vol. 65, No. 20, pp. 5783–5793, 2014
doi:10.1093/jxb/eru312 Advance Access publication 6 August, 2014

Journal of Experimental Botany
www.jxb.oxfordjournals.org

RESEARCH PAPER

Soil $H_2{}^{18}O$ labelling reveals the effect of drought on $C^{18}OO$ fluxes to the atmosphere

Matti Barthel[1,2,†], Patrick Sturm[2,*], Albin Hammerle[2,3], Nina Buchmann[2], Lydia Gentsch[2,5], Rolf Siegwolf[4] and Alexander Knohl[2,5]

[1] Ecosystems and Global Change, Landcare Research, P.O. Box 69040, Lincoln 7640, New Zealand
[2] Institute of Agricultural Sciences, ETH Zürich, Universitätsstrasse 2, 8092 Zurich, Switzerland
[3] Institute of Ecology, University of Innsbruck, Sternwartestrasse 15, 6020 Innsbruck, Austria
[4] Laboratory for Atmospheric Chemistry/Stable Isotopes & Ecosystem Fluxes, PSI – Paul Scherrer Institute, 5232 Villigen, Switzerland
[5] Chair of Bioclimatology, Georg-August University of Göttingen, Büsgenweg 2, D-37077 Göttingen, Germany

* Present address: TOFWERK AG, Uttigenstrasse 22, 3600 Thun, Switzerland.
† To whom correspondence should be addressed. E-mail: mbarthel@ethz.ch

Received 20 June 2014; Revised 20 June 2014; Accepted 23 June 2014

Abstract

Above- and belowground processes in plants are tightly coupled via carbon and water fluxes through the soil–plant–atmosphere system. The oxygen isotopic composition of atmospheric CO_2 and water vapour (H_2O_v) provides a valuable tool for investigating the transport and cycling of carbon and water within this system. However, detailed studies on the coupling between ecosystem components and environmental drivers are sparse. Therefore, we conducted a $H_2{}^{18}O$-labelling experiment to investigate the effect of drought on the speed of the link between below- and aboveground processes and its subsequent effect on $C^{18}OO$ released by leaves and soils. A custom-made chamber system, separating shoot from soil compartments, allowed separate measurements of shoot- and soil-related processes under controlled conditions. Gas exchange of oxygen stable isotopes in CO_2 and H_2O_v served as the main tool of investigation and was monitored in real time on *Fagus sylvatica* saplings using laser spectroscopy. $H_2{}^{18}O$-labelling showed that drought caused a slower transport of water molecules from soil to shoot, which was indicated by its direct derivation from independently measured concentrations and $^{18}O/^{16}O$ ratios of CO_2 and H_2O_v, respectively. Furthermore, drought reduced the ^{18}O equilibrium between H_2O and CO_2 at the shoot level, resulting in less-enriched $C^{18}OO$ fluxes from leaf to atmosphere compared with control plants. Compared with the shoot, ^{18}O equilibrium was not instantaneous in the soil and no drought effect was apparent.

Key words: Above/belowground, $C^{18}OO$, coupling, drought, *Fagus sylvatica*, $H_2{}^{18}O$, laser spectroscopy.

Abbreviations: $^{18}\Delta_{mea}$, measured discrimination against $C^{18}OO$; $^{18}\Delta_{mod\text{-}simple}$, modelled discrimination against $C^{18}OO$ without varying θ; $^{18}\Delta_{mod\text{-}extended}$, modelled discrimination against $C^{18}OO$ including varying θ; δ_A, $\delta^{18}O$ of CO_2 in atmosphere, equivalent to $\delta_{OUT\text{-}C}$; δ_E, $\delta^{18}O$ of water at the leaf evaporative front; δ_{ES}, $\delta^{18}O$ of water at the soil evaporative front; δ_{EV}, $\delta^{18}O$ of soil evaporation; δ_L, $\delta^{18}O$ of CO_2 dissolved in leaf water (assuming 100% equilibrium with δ_E); δ_{SR}, measured $\delta^{18}O$ of CO_2 flux from soil to atmosphere; $\delta_{SR\text{-}mod}$, modelled $\delta^{18}O$ of CO_2 flux from soil to atmosphere; $\delta_{IN\text{-}C}$, $\delta^{18}O$ of CO_2 at chamber inlet; $\delta_{IN\text{-}W}$, $\delta^{18}O$ of H_2O_v at chamber inlet; $\delta_{OUT\text{-}C}$, $\delta^{18}O$ of CO_2 at chamber outlet; $\delta_{OUT\text{-}W}$, $\delta^{18}O$ of H_2O_v at chamber outlet; δ_T, $\delta^{18}O$ carried by leaf transpiration; δ_V, $\delta^{18}O$ of water vapour in atmosphere, equivalent to $\delta_{OUT\text{-}W}$; ε^*, ε^*_{soil}, equilibrium fractionation between liquid water and water vapour at the air–water interfaces, for leaves and soil respectively; ε_k, kinetic fractionation during H_2O_v diffusion from the leaf intercellular airspaces to the atmosphere; $\varepsilon_{k\text{-}soil}$, kinetic fractionation during H_2O_v diffusion from the soil airspaces to the atmosphere; ε_w, equilibrium fractionation between H_2O and CO_2; θ, extent of ^{18}O equilibrium between H_2O and CO_2; ξ, ratio of CO_2 entering the chamber compared with the photosynthetic flux; A_N, net photosynthesis; $\bar{a}$, diffusive ^{18}O fractionation from atmosphere to leaf evaporative front; $\bar{a}_s$, diffusive ^{18}O fractionation from soil evaporative front to atmosphere; CA, carbonic anhydrase; C_a, atmospheric CO_2 concentration; C_c, CO_2 concentration at the site of carboxylation; C_{IN}, CO_2 mole fraction at chamber inlet; C_{OUT}, CO_2 mole fraction at chamber outlet, equal to C_a; E, leaf transpiration; E_s, soil evaporation; g_b, leaf boundary layer conductance to H_2O_v; g_s, stomatal conductance to H_2O_v; e_a, water vapour pressure in the atmosphere; e_i, water vapour pressure in the leaf, assuming water vapour saturation in the leaf; e_s,water vapour pressure in the soil, assuming water vapour saturation in the soil; $H_2{}^{18}O$, water enriched in ^{18}O (label); H_2O_v, water vapour; r, retroflux factor, i.e. factor by which leaf CO_2 retroflux exceeds photosynthetic flux A_N; R_s, soil respiration; SWC, soil water content; T_a, air temperature; T_l, leaf temperature; T_s, soil temperature; VPD, vapour pressure deficit; WVIA, water vapour isotope analyser; W_{OUT}, water vapour mole fraction at chamber outlet, equivalent to atmospheric H_2O_v; W_{IN}, water vapour mole fraction at chamber inlet.

Introduction

The biogeochemical cycling of carbon and water vapour between the terrestrial biosphere and the atmosphere makes terrestrial ecosystems a major player in Earth's climate system. The predicted higher probability/frequency of climate extremes (Schär *et al.*, 2004), such as droughts, has the potential to alter biogeochemical cycling in terrestrial ecosystems and hence to generate feedback within the climate system. In particular, soil drought is a major factor determining carbon and water fluxes through the soil–plant–atmosphere system (Granier *et al.*, 2007). Among other factors, soil drought controls stomata regulation (e.g. Gollan *et al.*, 1986), which in turn influences photosynthesis and transpiration. Soil drought also reduces the speed of link of carbohydrate allocation from above- to belowground ecosystem compartments, probably being limited by stomata-mediated carbon uptake and transfer (Rühr *et al.*, 2009; Barthel *et al.*, 2011*a*). Since soil drought affects the carbon-related speed of link from above- to belowground (phloem), soil drought might also affect the plant–soil coupling in the opposite direction, i.e. affecting the water-related speed of the link from below- to aboveground (xylem).

Analogous to ^{13}C (Kayler *et al.*, 2010), ^{18}O in water can serve as a tool to investigate plant physiology and soil–plant coupling, i.e. the speed of the link from below- to aboveground. Moreover, the ^{18}O-composition of soil or leaf water should immediately be passed on to CO_2, as dissolved CO_2 exchanges its oxygen isotopic signature with water. In leaves, the equilibrium reaction between CO_2 and H_2O is catalysed by the enzyme carbonic anhydrase (CA) (Silverman 1982; Gillon and Yakir 2000*a*, 2001), whereas in soils such CA activity is still under debate (Tans, 1998; Seibt *et al.* 2006; Wingate *et al.*, 2008). As water concentrations are usually much higher than those of CO_2, water will always impose its oxygen isotopic ratio upon the dissolved CO_2, irrespective of the initial isotopic signature of CO_2 (Miller *et al.*, 1999). Consequently, CO_2 molecules that diffuse from leaves or soils should carry the oxygen isotopic signature of leaf or soil water, respectively. Thus, any change in the soil water oxygen isotopic composition will propagate within the soil–plant–atmosphere system, and eventually affect the oxygen stable isotope composition of atmospheric CO_2 (δ_A). δ_A in turn is one of the few tools to separate the major terrestrial ecosystem CO_2 gross fluxes, photosynthesis and respiration, into their net components at global (Ciais *et al.*, 1997) or local (Kato *et al.*, 2004; Sturm *et al.*, 2012) scales. Similarly, Bowling *et al.* (2003) utilized the oxygen stable isotope difference between soil and leaves to quantify the relative contribution of soil and foliar respiration to total nocturnal ecosystem respiration. However, using δ_A in order to separate assimilatory from respiratory fluxes at subdaily time scales requires a detailed understanding of how rapid changes of soil or leaf water ^{18}O (for instance due to rain events or strong evaporative enrichment) translate to $C^{18}OO$ fluxes from individual ecosystem components—especially under different environmental conditions such as drought. Yakir (2003) stated that the $\delta^{18}O$ value of precipitation is the single most important environmental control on δ_A, as it translates to soil water and feeds plants. He further pointed out that, at the global scale, it is the leaf and soil components that dominate the uncertainty of the global ^{18}O mass balance. Although there are a considerable number of studies on $C^{18}OO$ fluxes in terrestrial ecosystems where individual components were investigated, such as the soil atmosphere $C^{18}OO$ flux (Miller *et al.*, 1999; Wingate *et al.*, 2008) or the canopy-to-atmosphere flux (Griffis *et al.*, 2011), research on the link between components has so far been neglected.

Thus, we conducted a $H_2{}^{18}O$-labelling experiment to investigate the effect of drought on the speed of the link between below- and aboveground processes and its subsequent effect on $C^{18}OO$ released by leaves and soils. We hypothesized that ^{18}O-labelling (watering) would result in a continuous enrichment of soil and leaf waters, which in turn would change the ^{18}O composition of CO_2 released to the atmosphere (Fig. 1). We expected that $H_2{}^{18}O$ label-induced enrichment in the shoot compartment would be time lagged, given the transport times within the plant. As stomatal conductance is generally downregulated during drought, we further hypothesized that water molecule transport from soil to shoot would be reduced under drought conditions, hence also delaying the enrichment of ^{18}O in CO_2. In order to trace the ^{18}O flux on an hourly timescale, gas exchange in the soil and shoot was measured in real time using online laser spectroscopy. To our knowledge, this is the first study reporting on measuring, concurrently and continuously, the $^{18}O/^{16}O$ ratio in CO_2 and water vapour (H_2O_v) of shoot and soil gas exchange after irrigation of the soil surface with ^{18}O-labelled water.

Materials and methods

Experimental design and set-up

The experiment was carried out in a growth cabinet using small beech saplings (*Fagus sylvatica* L., height approx. 1 m, n=6). The

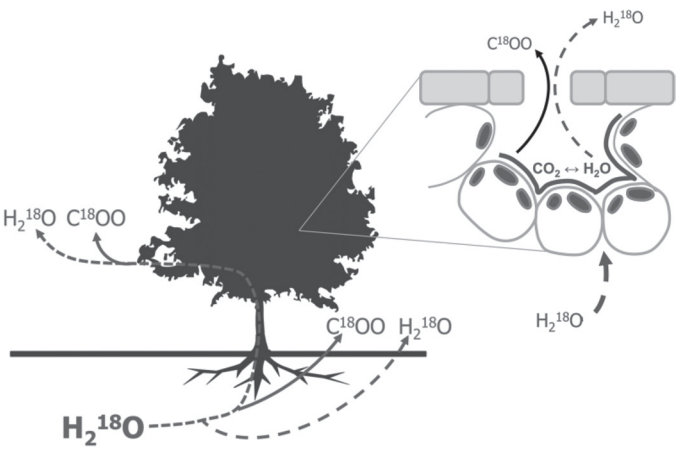

Fig. 1. Schematic overview of the methodological approach. $H_2{}^{18}O$ labelling enabled us to investigate the effect of drought on the speed of the link between below- and aboveground processes by tracing ^{18}O from soil to leaf water, and to investigate its subsequent effect on $C^{18}OO$ released by leaves and soils. Insert: Schematic traverse section of the substomatal cavity in a deciduous leaf: CA facilitates the exchange of oxygen isotopes between water and dissolved CO_2 at the evaporative front in leaves. Therefore, CO_2 which retrodiffuses from the leaf back to the atmosphere (the proportion of CO_2 that has not been used for photosynthesis) is naturally enriched in ^{18}O compared with atmospheric CO_2.

growth cabinet was set to a constant day/night cycle (18–22 °C) with a light period of 15 h. The highest light intensity was programmed between 10 a.m. and 6 p.m. with a maximal photosynthetic active radiation of 600 µmol m^{-2} s^{-1}. Gas exchange was monitored using six custom-made soil/shoot chambers, which entirely enclosed the shoot and soil compartment of each beech sapling (soil chamber cylinder: length=250 mm, diameter=297mm, volume=17.7 l; shoot chamber cylinder: length=800 mm, diameter=292 mm, volume=56.6 l). A gas-tight separation between both chamber compartments enabled an independent measurement of above- and belowground gas exchange. Each combined soil/shoot chamber was equipped with sensors for relative humidity, soil moisture, and air, leaf, and soil temperature. Two fans inside each shoot chamber ensured air mixing within the respective canopy. Soil and shoot chambers were continuously flushed in order to maintain steady-state conditions. Air subsamples were taken from the chamber outlets and directed to laser spectrometers, which quantified mixing ratios and the isotopic composition of CO_2 and H_2O_v at a rate of 0.5 Hz. The respective chamber inlets and outlets were measured alternately for 140 s each, of which the average was used for further calculations. All chambers were measured successively within a continuous measurement sequence. Three replicates were subjected to drought, and the remaining three replicates served as controls. The measurement set-up resulted in a temporal resolution of one measurement h^{-1} of each soil and shoot subdivision of all six chambers. Real-time data acquisition/processing as well as the control of instruments, calibration units, chambers, valves and sensors was accomplished with a custom-written LabVIEW program (LabVIEW, National Instruments, Austin, TX, USA). For more details on the entire measurement set-up, see Barthel *et al.* (2011*b*). Gas-exchange parameters such as photosynthesis and transpiration were calculated according to von Caemmerer and Farquhar (1981).

Instrumentation

Oxygen stable isotope ratios are reported relative to the Vienna Standard Mean Ocean Water scale (V-SMOW) using the δ notation (‰):

$$\delta^{18}O = \frac{R_{sample}}{R_{V\text{-}SMOW}} - 1 \quad (1)$$

where R_{sample} and $R_{V\text{-}SMOW}$ denote the $^{18}O/^{16}O$ ratio of the sample and the standard, respectively.

CO_2 isotope analyser A commercially available pulsed quantum cascade laser absorption spectrometer (Aerodyne Research, Billerica, MA, USA) was used to simultaneously measure the CO_2 isotopologues $^{12}C^{16}O_2$, $^{13}C^{16}O_2$, and $^{12}C^{16}O^{18}O$ at a rate of 0.5 Hz by scanning across three spectral lines near 4.3 µm (2310 cm^{-1}). The measurement was based on two optical multiple pass absorption cells with stabilized pressure and temperature using a spectral ratio method (Nelson *et al.*, 2008). Furthermore, the laser system was equipped with an infrared detector cooled with liquid nitrogen. System operation was fully automated using an automated liquid nitrogen refilling device (liquid N_2 Microdosing system #905; Norhof, Maarssen, The Netherlands) and a self-made calibration unit. Throughout the measurement sequence, calibration was done approximately once h^{-1} for 6 min in three consecutive steps. First, a dilution calibration was performed to correct for the instrument's non-linear CO_2 concentration dependence of isotope ratio measurements. Secondly, two calibration gases with known mixing ratios were measured for a two-point calibration. Thirdly, a quality-control standard gas was measured to check the long-term stability of the calibrated instrument. The 1σ standard deviation of repeated quality-control standard measurements was ±0.23‰ for $\delta^{18}O$ and ±0.09 ppm for CO_2 concentrations. A detailed description of the quantum cascade laser absorption spectrometer calibration strategy and system operation can be found in Sturm *et al.* (2012).

Water vapour isotope analyser A commercially available water vapour isotope analyser (WVIA; DLT-100, Los Gatos Research, Mountain View, CA, USA), based on off-axis integrated cavity output spectroscopy, was used for the simultaneous measurement of the three water isotopologues $H_2{}^{16}O$, $H_2{}^{18}O$, and $^2H^1H^{16}O$. The laser scanned over three nearby absorption lines at a wavelength of ~1.389 µm. The WVIA was calibrated using a self-made calibration system involving a piezoelectric droplet generator. The 1σ standard deviation of repeated quality-control standard measurements was ±0.23‰ for $\delta^{18}O$ and ±92 ppm for H_2O_v concentrations. For more information on the WVIA, see Sturm and Knohl (2010).

As H_2O_v concentration measurements are prone to condensation events, WVIA measurements at the shoot chamber outlets were verified by modelling H_2O_v concentrations within the shoot chamber using sensors for air temperature and relative humidity (Buck, 1981). In general, very good agreement between both approaches was observed (Fig. 2). However, at very high H_2O_v concentrations (>22 000 ppm), the linear relationship was lost, which may point to condensation events during these measurements. The effect of condensation on the ^{18}O measurements would have underestimated the enrichment by a maximal 2‰, which is minor considering the strong label intensity (see Supplementary information at *JXB* online for derived error estimation). Note that this error affected mainly control measurements, since transpiration and thus relative humidity inside the shoot chambers were higher. As air temperature and relative humidity were only measured in the shoot chambers, such independent verification could not be done for soil chamber H_2O_v measurements.

Watering with labelled water ($H_2{}^{18}O$)

Prior to $H_2{}^{18}O$ application, soils of three replicates were gradually dried during approximately 20 d before the start of the experiment. Once plants achieved the desired stress level, about 30 ml of water was added daily to maintain the stress and prevent mortality. At the label day, all soils were simultaneously irrigated with 400 ml of ^{18}O-labelled water ($\delta^{18}O$=449 ± 7‰) at 11 a.m. to induce a sudden change in $\delta^{18}O$ value of soil water. For comparison, the $\delta^{18}O$ of

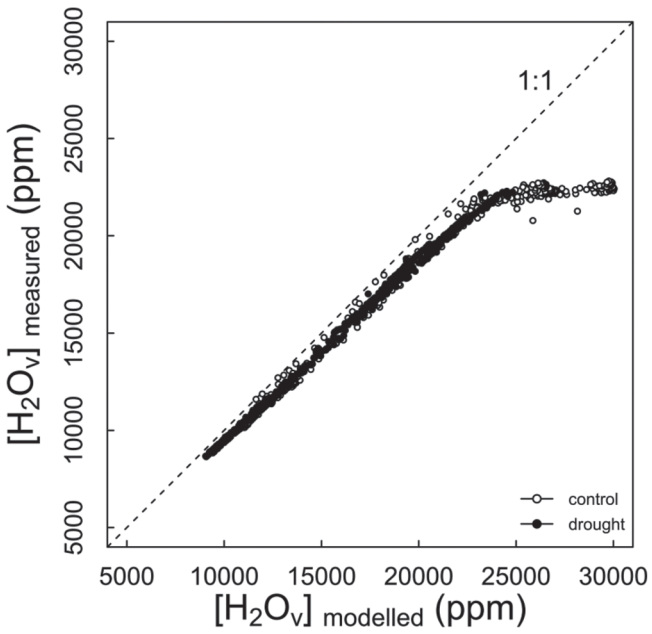

Fig. 2. Relationship between water vapour concentrations modelled from air temperature and the relative humidity sensor inside the shoot chamber and directly measured water vapour concentrations. Control treatment is shown by open symbols, drought treatment by closed symbols, and *x=y* by a dashed line.

local tap water used for regular daily irrigation was –11.05 ± 0.24‰. Subsequent to the $H_2{}^{18}O$ watering, the change in $^{18}O/^{16}O$ of CO_2 and H_2O_v fluxes was monitored in shoot and soil compartments of each replicate using the isotope gas-exchange data from both the WVIA and the CO_2 isotope analyser.

Data processing

Since replicates were measured successively, the data were half-hourly linearly gap filled in order to achieve consistent time intervals for averaging. By averaging the gap-filled data, a single timeline could be obtained. Because of disturbance effects during label application, isotope data for this time period (1 h) was removed from further analysis. H_2O_v measurements were filtered according to plausibility ($W_{OUT} - W_{IN}>0$ must be true, where W_{OUT} is water vapour mole fraction at the chamber outlet, equivalent to atmospheric H_2O_v, and W_{IN} is the water vapour mole fraction at the chamber inlet). Moreover, isotope data were filtered for daytime values only, as night-time measurements were prone to condensation in the tubing because of lower temperatures in the growth cabinets. All data were analysed and processed using the statistical software R 2.15.1 (R Development Core Team, 2011). Results are always shown as the mean±standard error (SE) (n=3) per treatment.

Isotope modelling

In order to assess the ^{18}O equilibrium at leaf and soil levels, directly measured ^{18}O in CO_2 was compared with the theoretically expected values, which can be modelled from ^{18}O measurements in H_2O_v.

Leaf component The isotopic composition of leaf water ^{18}O at the evaporative front (δ_E) is generally enriched compared with the source water (Gonfiantini *et al.*, 1965), depending on the gradient between atmospheric water vapour pressure (e_a) and the water vapour pressure within the leaf (e_l). Assuming non-steady-state conditions, leaf water enrichment at the evaporative front can be modelled as:

$$\delta_E = \delta_T + \varepsilon^* + \varepsilon_K + (\delta_V - \delta_T - \varepsilon_K)\frac{e_a}{e_l} \quad (2)$$

The equation is based on a model of evaporative enrichment by Craig and Gordon (1965), originally developed for free water surfaces, where δ_T and δ_V are the isotopic composition of the transpirational flux and of atmospheric water vapour, respectively. Replacing source water $\delta^{18}O$ with δ_T allows the assessment of δ_E under non-steady-state conditions (Harwood *et al.*, 1998; Gillon and Yakir, 2000*b*). This assumption is essential for our set-up as the isotopic composition of source water is constantly changing after labelling with $H_2{}^{18}O$. Modelling leaf water enrichment at the evaporative front usually also accounts for the Péclet effect. The Péclet effect describes the convection of unenriched leaf vein water towards the evaporative sites, hence counteracting evaporative enrichment (Farquhar and Lloyd, 1993; Cernusak and Kahmen, 2013). However, since a strong ^{18}O label was used for watering, we assumed the Péclet effect to be negligible in modelling δ_E. The parameter ε_K in Eqn (2) denotes the kinetic fractionation during water vapour diffusion from the leaf intercellular airspaces to the atmosphere, and is obtained from the relative contributions of leaf stomatal (g_s) and leaf boundary layer conductance to H_2O_v (g_b, set constant to 1.42 mol m^{-2} s^{-1}; Luz *et al.*, 2009):

$$\varepsilon_K = \frac{28g_s^{-1} + 22g_b^{-1}}{g_s^{-1} + g_b^{-1}}. \quad (3)$$

The equilibrium fractionation ε^* between liquid water and water vapour at the air–water interfaces is expressed as a function of leaf temperature (T_l, in Kelvin) according to Horita and Wesolowski (1994):

$$\varepsilon^* = -7.685 + 6.7123\left(\frac{10^3}{T_l}\right) - 1.6664\left(\frac{10^6}{T_l^2}\right) + 0.35041\left(\frac{10^9}{T_l^3}\right). \quad (4)$$

The $\delta^{18}O$ signal of transpiration fluxes (δ_T) was calculated using an isotopic mass balance equation:

$$\delta_T = \frac{\delta_{OUT-W}W_{OUT} - \delta_{IN-W}W_{IN}}{W_{OUT} - W_{IN}}, \quad (5)$$

where W_{IN} and W_{OUT} denote the respective mole fractions at chamber inlet and outlet. Similarly, $\delta_{IN\text{-}W}$ and $\delta_{OUT\text{-}W}$ denote the respective ^{18}O isotopic compositions of H_2O_v at chamber inlet and outlet.

According to theory, leaf or soil water ^{18}O composition is passed on to CO_2 due to the following isotopic equilibrium reaction of CO_2 with H_2O:

$$H_2{}^{18}O_{(l)} + CO_{2(g)} \leftrightarrow H^+ + \left[HCO_2{}^{18}O\right]^-_{(aq)} \leftrightarrow H_2O_{(l)} + CO^{18}O_{(g)}.$$

In leaves, the reaction is catalysed by the enzyme CA, which facilitates CO_2 hydration and ^{18}O exchange. Assuming full CA-catalysed isotopic equilibrium of CO_2 with leaf water, the water oxygen isotopic composition at the evaporative front (δ_E) should correspond directly to that of dissolved CO_2, when accounting for the equilibrium fractionation between H_2O and CO_2. This oxygen isotopic equilibrium is expressed by:

$$\delta_L = \delta_E + \varepsilon_W, \quad (6)$$

$$\text{with } \varepsilon_W = \frac{17604}{T_l} - 17.93, \quad (7)$$

where δ_L is the oxygen stable isotope composition of CO_2 at the evaporative front and ε_W is the equilibrium fractionation between H_2O and CO_2 (Brenninkmeijer *et al.*, 1983). Based on this assumption, the theoretical discrimination ($^{18}\Delta_{mod\text{-}simple}$) can be modelled by accounting for the weighed mean of diffusive ^{18}O fractionations occurring during CO_2 diffusion out of the leaf ($\bar{a}$=7.4‰) and the retroflux r following Farquhar *et al.* (1993):

$${}^{18}\Delta_{mod-simple} = \bar{a} + r(\delta_L - \delta_A) \quad (8)$$

Farquhar *et al.* (1993) described the retroflux factor r mathematically as $r=C_c/(C_a - C_c)$, where C_a and C_c denote the CO_2 concentration in the atmosphere and at the site of carboxylation, respectively. This equation illustrates that an estimation of r is challenging, as it requires a very good estimate of stomata as well as mesophyll conductance to CO_2, since they determine the magnitude of C_c and hence r. However, a precise estimate of C_c was not possible with this experimental set-up. Therefore, a sensitivity analysis was done across a range of different r values. The r sensitivity analysis was based on the general assumption that only one-third of the CO_2 that diffuses into the leaf is consumed by photosynthesis (Ciais *et al.*, 1997; Tans, 1998; Yakir and Sternberg, 2000; Yakir, 2003). Therefore, the range of r was chosen to be between 1.9 and 2.1. In addition, a second sensitivity analysis was conducted where the original model from Farquhar *et al.* (1993) was extended to account for θ, the extent of ^{18}O equilibrium between H_2O and CO_2, which can range between 0 and 1, implying a 0–100% isotopic equilibrium, respectively (Yakir, 2003):

$${}^{18}\Delta_{mod-extended} = \bar{a} + r\left[\Theta_{eq}(\delta_L - \delta_A) - (1 - \Theta_{eq})\bar{a}/(r+1)\right] \quad (9)$$

Finally, $^{18}\Delta$ can be also obtained from direct measurements of ^{18}O in CO_2 following Evans *et al.* (1986):

$$^{18}\Delta_{mea} = \frac{\xi(\delta_{OUT\text{-}C} - \delta_{IN\text{-}C})}{1000 + \delta_{OUT\text{-}C} - \xi(\delta_{OUT\text{-}C} - \delta_{IN\text{-}C})}, \quad (10)$$

$$\text{with } \xi = \frac{C_{IN}}{(C_{IN} - C_{OUT})}, \quad (11)$$

where ξ is the ratio of CO_2 entering the chamber compared with the photosynthetic flux with C_{IN} and C_{OUT} denoting the respective CO_2 mole fractions at chamber inlet and outlet and $\delta_{IN\text{-}C}$ and $\delta_{OUT\text{-}C}$ the corresponding ^{18}O isotopic compositions of CO_2 at chamber inlet and outlet.

Soil component The isotopic composition of soil water at the evaporative surface (δ_{ES}) was calculated in accordance with Eqn (2). To calculate the soil equilibrium fractionation factor (ε^*_{soil}) and the saturation water vapour pressure in the soil (e_s), leaf temperature was substituted by soil temperature. Soil kinetic fractionation, $\varepsilon_{k\ soil}$ was set constant at 28.5‰ after Merlivat (1978). The δ value of soil respiration ($\delta_{SR\text{-}mod}$) was modelled assuming a 100% equilibration of ^{18}O between soil H_2O and CO_2 using δ_{ES} and a soil kinetic fractionation ($\bar{a}_s$) of 8.8‰ according to Miller *et al.* (1999):

$$\delta_{SR-mod} = \delta_{ES} + \varepsilon_{ws} - \bar{a}_s \quad (12)$$

with ε_{ws} calculated according to Eqn (7) using soil temperature. Finally, soil evaporation (δ_{EV}) and soil respiration fluxes (δ_{SR}) were calculated according to Eqn (5) using data from H_2O_v and CO_2, respectively.

Results

Experimental pre-requisites and conditions before water addition

The analysis presented here is based upon the assumption that δ_T reflects the δ value of source water, which should hence be close to the δ value used for daily irrigation. Figure 3 shows the diurnal cycle of δ_T for control and drought treatment during the pre-label day. During the period of highest light intensity (10 a.m. to 6 p.m.), δ_T was slightly more enriched than tap water (11.05 ± 0.24‰) with marginally more enrichment

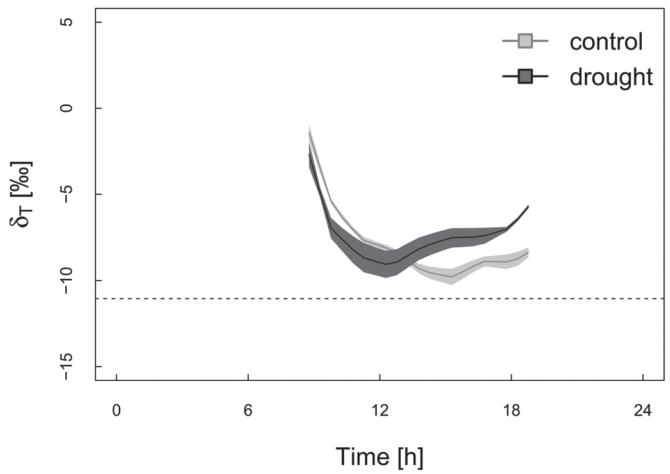

Fig. 3. Mean diurnal cycle of $\delta^{18}O$ in the transpirational flux (δ_T) during the pre-label day; means for control and drought treatments are shown by grey and black lines, respectively. Uncertainty is given as ±SE of the mean (shaded areas). For comparison, the $\delta^{18}O$ of local tap water used for regular daily irrigation was −11.05 ± 0.24‰ (dashed horizontal line).

in drought treatments during the afternoon. This relatively small deviation of measured δ_T from tap water values showed that δ_T approximately reflected source water values. The slightly more enriched δ_T value under drought conditions was probably caused by a stronger evaporative enrichment of soil water (source water).

Programmed diel cycles for the growth cabinets resulted in comparable diel cycles for soil and air temperatures across treatments (Fig. 4K, L). Before adding $H_2{}^{18}O$ to the soil, soil water content (SWC) of drought treatments was approximately 25% lower than that of control treatments. Withholding water reduced soil respiration (R_s) to 48%, photosynthesis (A_N) to 30%, evaporation (E_s) to 83%, and transpiration (E) to 37% compared with control values during the period of highest light intensity (Fig. 4A–D). Vapour pressure deficit (VPD) remained constantly higher in drought treatment, even after watering, but the diel cycle became less resolved (Fig. 4J).

Effect of drought on the speed of link between below- and aboveground processes

$H_2{}^{18}O$ labelling resulted in an immediate increase in SWC (Fig. 4I). Concurrently, a distinct enrichment in $\delta^{18}O$ values of soil evaporation (δ_{EV}; Fig. 4E) and soil respiration (δ_{SR}; Fig. 4G) was observed across treatments. The δ_{EV} of drought treatments increased rapidly to 412‰, which closely mirrors the δ value of the water used for labelling ($\delta^{18}O$=449 ± 7‰). In contrast, the maximum δ_{EV} of control treatments reached only ~304‰, probably due to dilution effects caused by the higher SWC. Over the course of the experiment, δ_{EV} decreased to about 122‰ (control) and 134‰ (drought), probably due to mixing effects with non-labelled soil water. Furthermore, soil respiration increased above pre-labelling levels in both treatments (Fig. 4A).

In the shoot, a coincident increase in A_N and g_s was apparent in drought treatments instantly after labelling, whereas the control showed no consistent response (Fig. 5A, B). However, this initial watering response of A_N and g_s levelled out after 1.5 h and accounted only for a 12% (A_N) and 16% (g_s) increase compared with the control. To quantify the speed of the link between above- and belowground, $^{18}\Delta_{mea}$ and δ_T were used as independent proxies, taking advantage of their direct derivation from independently measured concentrations and $^{18}O/^{16}O$ ratios of CO_2 and H_2O_v, respectively (Eqns 5 and 10). Both treatments displayed a delayed but exponential label-induced ^{18}O enrichment in the transpirational flux (δ_T), with a faster increase in control compared with drought treatments (Fig. 5C). Likewise, shoot discrimination against $C^{18}OO$ ($^{18}\Delta_{mea}$) showed a faster exponential increase in control compared with drought after labelling (Fig. 5D).

Effect of $H_2{}^{18}O$ labelling on $C^{18}OO$ released by soils and leaves

Figure 6A shows that the modelled δ value of soil respiration ($\delta_{SR\text{-}mod}$) was mostly overestimating measured δ_{SR}, especially during the pre-label and label day. During the pre-label day, δ_{SR} was only 61 ± 2% of $\delta_{SR\text{-}mod}$ in both treatments. During the label day, exchange constantly increased, which resulted

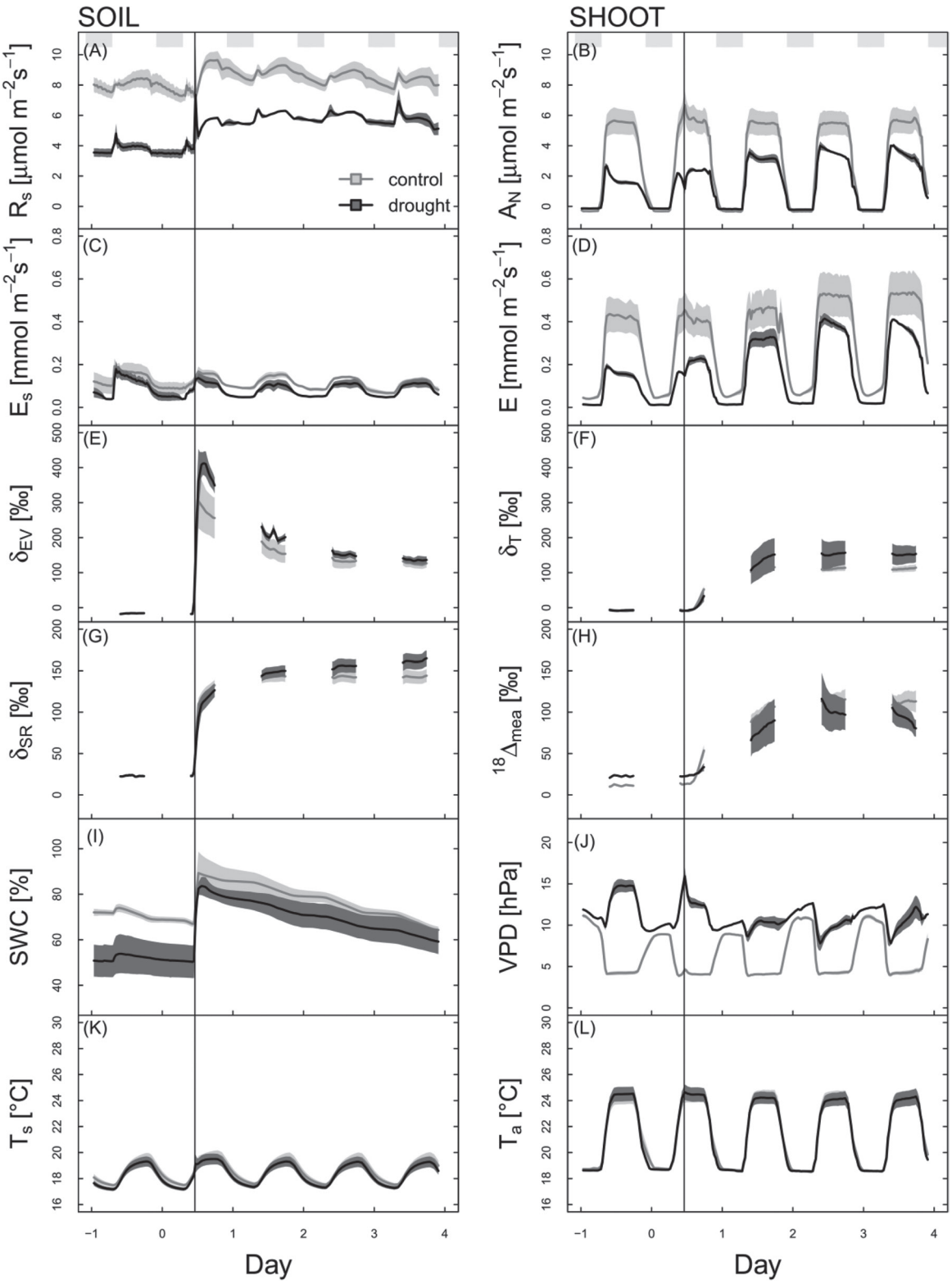

Fig. 4. Mean diel cycles of soil-related parameters (left panels) and shoot-related parameters (right panels) during the $H_2{}^{18}O$-labelling (vertical black line) experiment for (A) soil respiration (R_s); (B) photosynthesis (A_N); (C) evaporation from soil (E_s); (D) transpiration from shoot (E); (E) $\delta^{18}O$ of soil evaporation (δ_{EV}); (F) $\delta^{18}O$ of the transpirational flux (δ_T); (G) $\delta^{18}O$ of soil respiration (δ_{SR}); (H) discrimination against $C^{18}OO$ at the shoot ($^{18}\Delta_{mea}$); (I) relative volumetric soil water content (SWC); (J) vapour pressure deficit (VPD); (K) soil temperature (T_s); and (L) air temperature in shoot chamber (T_a). Means for control and drought treatments are shown by grey and black lines, respectively; uncertainty is given as ±SE of the mean (shaded areas); night-time is indicated as grey bars at the top of plot area.

in a better agreement between $\delta_{SR\text{-}mod}$ and δ_{SR} from post-label d 1–3. However, also at post-label d 1–3, substantial variations around the 1:1 line were still observed, either under- or overestimating δ_{SR} by about 50‰ (Fig. 6B).

In the shoot, modelled discrimination against $C^{18}OO$, based on leaf water enrichment ($^{18}\Delta_{mod\text{-}simple}$; $^{18}\Delta_{mod\text{-}extended}$) predicted very well the measured discrimination against $C^{18}OO$ ($^{18}\Delta_{mea}$). A strong linear relationship between $^{18}\Delta_{mod}$

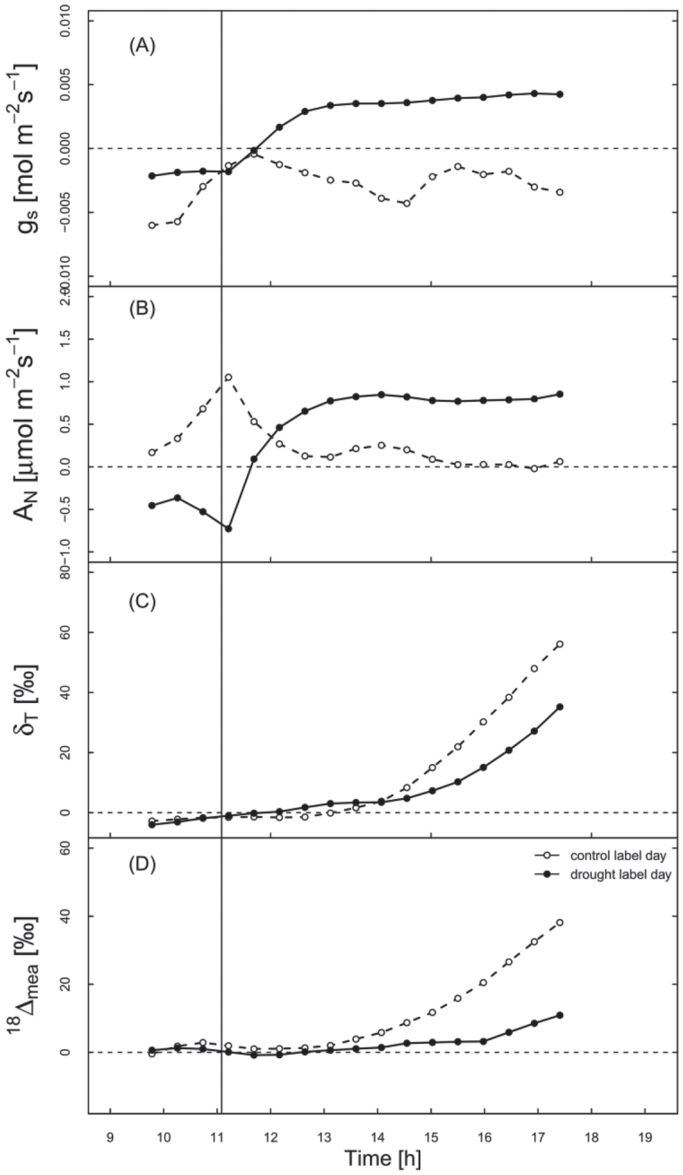

Fig. 5. Immediate response during the label day in quantitative differential to the preceding non-label day for: (A) stomatal conductance (g_s); (B) photosynthesis (A_N); (C) $\delta^{18}O$ of the transpirational flux (δ_T); and (D) measured discrimination against $C^{18}OO$ at the shoot level ($^{18}\Delta_{mea}$). $H_2{}^{18}O$ labelling is shown by a vertical black line, control treatment by open symbols, drought by closed symbols, and zero by a horizontal dashed line.

and $^{18}\Delta_{mea}$ was found for both treatments during the label day (Fig. 7). The slopes between $^{18}\Delta_{mod}$ and $^{18}\Delta_{mea}$ gave an indication of the extent of ^{18}O equilibrium at the shoot level. The data suggested that drought reduced the ^{18}O exchange between CO_2 and H_2O, as the relationship between $^{18}\Delta_{mod}$ and $^{18}\Delta_{mea}$ showed steeper slopes for the control across a given range of r or θ. Choosing r=1.9, 2.0, and 2.1 and θ=1 resulted in respective slopes of 1.04, 0.99, and 0.95 in the control treatment and 0.27, 0.26, and 0.24 in the drought treatment (Fig. 7A). On the other hand, choosing θ=1, 0.75, and 0.5 and r=2.0 resulted in respective slopes of 0.99, 1.32, and 1.99 in the control treatment and 0.26, 0.34, and 0.51 in the drought treatment (Fig. 7B). Hence, reducing θ to 0.5 with r=2.0 caused a doubling in slope. All regressions showed R^2>0.97 and P<0.001. Note that a decrease of r under drought conditions would produce an increase in the slope but also unrealistic results, as a certain proportion of the values would fall above the 1:1 line, hence implying an unrealistic exchange of more than 100%. On the other hand, increasing r would result in even smaller slopes under drought conditions. In conclusion, under realistic conditions, slopes were always lower in the drought compared with the control treatment at any given r or θ.

Discussion

In soils, the increased ^{18}O signal caused by labelling was not transferred instantaneously from H_2O to CO_2, which was reflected in the poor agreement between the modelled and measured isotopic signature of soil respiration. This discrepancy between modelled and measured values is most likely due to the simple model approach used assuming instantaneous exchange and constant kinetic fractionation. In the following, we will discuss the importance of these two model parameters on our results.

We assumed an instantaneous exchange at the soil level since recent field studies found a considerable CA activity in soils, evidenced by instantaneous ^{18}O exchange in soils (Seibt *et al.*, 2006; Wingate *et al.*, 2008) and carbonyl sulfide uptake from soils (Kesselmeier *et al.*, 1999; Kesselmeier and Hubert, 2002). Such instantaneous equilibrium in soils would be in line with the common instantaneous exchange in plant leaves. However, this subject is far from settled. In principle, ^{18}O exchange between CO_2 and H_2O is just a function of temperature (Tans, 1998) and occurs only after hydration of the dissolved CO_2 to carbonic acid (Mills and Urey, 1940) with a rate constant of 0.012 s^{-1} (Skirrow, 1975; Tans, 1998). Apart from soil water, Stern *et al.* (1999) found that the isotopic signature of soil CO_2 is mainly influenced by the rate constant of the isotopic exchange but also by soil-filled pore space and tortuosity. The latter two are mainly interfering with the kinetic fractionation from diffusion, and thus dry soils are likely to produce different kinetic fractionation compared with wet soils. To avoid underestimation of this effect, we assumed a maximal theoretical value of 8.8‰ (Miller *et al.*, 1999) in both treatments. Several earlier works have elaborated on the correct prediction of the isotopic signature of soil CO_2 including effects related to the invasion flux from atmosphere to soil (Stern *et al.*, 2001), effects from the soil water bound to soil surfaces (Miller *et al.*, 1999), or effects from the near surface gradient of soil water ^{18}O (Riley, 2005). Thus, predicting δ_{SR} under different environmental conditions is complex as it involves a number of physical and chemical uncertainties that are hard to quantify. The labelling approach did not result in significant differences between dry and wet soils, although a strong isotopic shift was induced. Considering the time it took until a new isotopic equilibrium was established let us suggest that ^{18}O equilibrium was not instantaneous in soils, which in turn points to a reduced CA activity. However, the extent of CA reduction within soils cannot be deduced from the data, and additional experiments are needed.

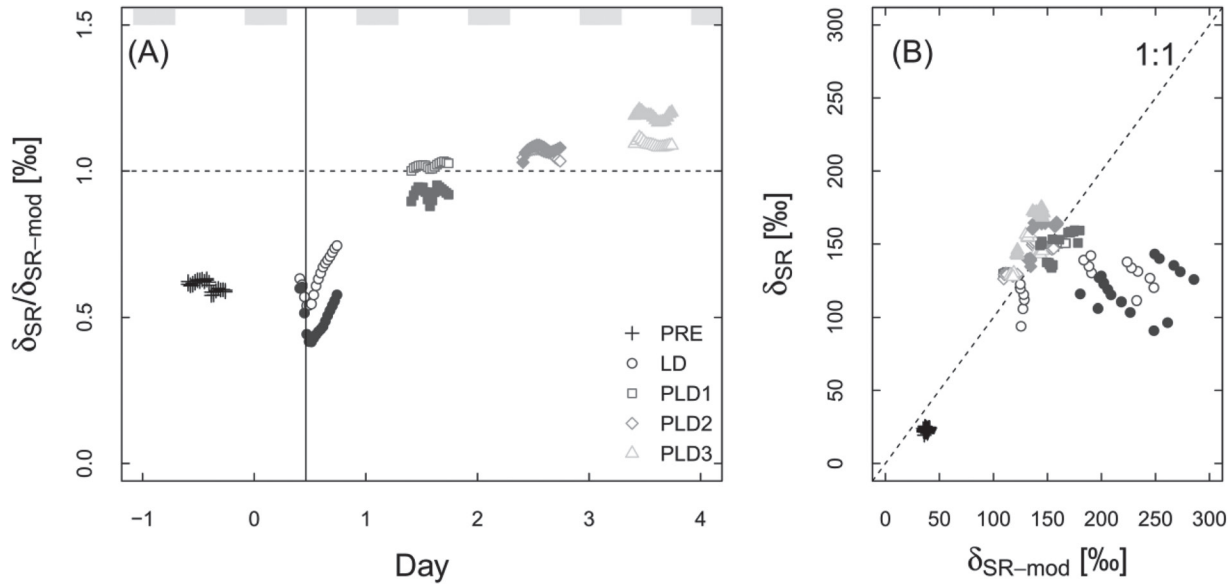

Fig. 6. (A) Ratio between the $\delta^{18}O$ of modelled soil respiration ($\delta_{SR\text{-}mod}$) based on δ_{EV} and the measured $\delta^{18}O$ of soil respiration (δ_{SR}) over the course of the experiment. Data shown are mean half-hourly values from each treatment. (B) Corresponding relationship between $\delta_{SR\text{-}mod}$ and δ_{SR}. Control treatment is shown by open symbols, drought treatment by closed symbols, and *x=y* by a dashed line. PRE, pre-label day; LD, label day; PLD, post-label day. Data shown are individual measurements from each treatment.

In the shoot, $H_2{}^{18}O$ labelling caused a rapid increase of A_N and g_s of drought treatments within 30 min. Such a fast ecophysiological response is in strong accordance with an irrigation experiment done in a Swiss forest with 115-year-old beech trees, where a rapid response (within 6 min) of the xylem sap flow rate was measured upon irrigation of previously drought-stressed trees (Cermak *et al.*, 1993). A similar response has been also described for 3- to 6-month-old *Eucalyptus pauciflora* saplings, where a fast response of A_N and g_s to rewatering within 5–60 min was identified after drought (Kirschbaum, 1988). Moreover, our observed rapid reaction of A_N and g_s was not accompanied by the arrival of labelled water molecules, which occurred later. Furthermore, δ_T and $^{18}\Delta$ showed independently that drought also delayed the transport of water from below- to aboveground, thus affecting the ^{18}O signal propagation from soil to shoot. The observed, slightly higher stomatal conductance after $H_2{}^{18}O$ labelling could therefore not compensate for the slower movement of molecules through the xylem. A reduced sap flow under drought conditions has also been confirmed in field studies for *Fraxinus excelsior* L. (Stöhr and Lösch, 2004), *Betula pendula*, and *Picea abies* (Gartner *et al.*, 2009). According to Nadezhdina (1999), sap flow can even be used as a proxy for whole-plant water status.

Upon arrival of labelled H_2O molecules in the shoot, almost instantaneous ^{18}O exchange between H_2O and CO_2 was found in both treatments as had been indicated by a strong relationship between $^{18}\Delta_{mod}$ and $^{18}\Delta_{mea}$. According to the theory, instantaneous ^{18}O equilibrium between H_2O and CO_2 is facilitated by CA. CA is ubiquitous in leaves and found predominantly in leaf chloroplasts, which are generally located (to facilitate gas exchange) close to the sites of evaporative enrichment (Yakir, 2003). Furthermore, CA has a turnover rate of up to 10^6 s^{-1}, which is one of the fastest known enzymatic reactions (Silverman, 1982). In the 1990s, studies on δ_A generally assumed a full isotopic equilibrium between CO_2 and H_2O for both leaves and soil (Francey and Tans, 1987; Farquhar *et al.*, 1993; Yakir and Wang, 1996; Ciais *et al.*, 1997), which was then fundamentally refuted by Gillon and Yakir (2001). They showed marked differences among different plant taxa and physiological groups, resulting in an overall global weighed mean with θ=0.78. Among groups, C_3 plants showed the highest equilibrium rates with θ>0.95 in 26 out of 39 species. This was contrasted by a θ of only 0.38 in C_4 grasses (Gillon and Yakir, 2000*a*, 2001). In C_3 trees, an average θ was estimated at 0.93, which is similar to the range observed in this study under control conditions for beech (0.93–0.98). After the paper by Gillon and Yakir (2001), a number of papers confirmed these findings. For instance, Cernusak *et al.* (2004) estimated θ in *Ricinus communis* during leaf dark respiration and photosynthesis at 0.8 and 1, respectively. However, Edwards *et al.* (2007) showed that the low CA activity in C_4 grasses could also be a characteristic physiological trait of the PACCAD clade of grasses, which also include C_3 grasses.

The data presented here suggest that drought reduces the ^{18}O exchange between CO_2 and H_2O at the shoot level across a range of different retroflux intensities and θ values. The reduced extent of ^{18}O equilibrium under drought is in accordance with Guliyev *et al.* (2008), who found a reduction in CA activity after a long drought period in wheat. Among potential environmental influences on CA activity, so far only irradiation has been shown to have an effect on the hydration efficiency in leaves, as shown by Cousins *et al.* (2006). Since an integrated shoot approach was chosen in our study for estimating the extent of ^{18}O equilibrium at the shoot level, intraleaf variations of CA activity as observed in *Zea mays*

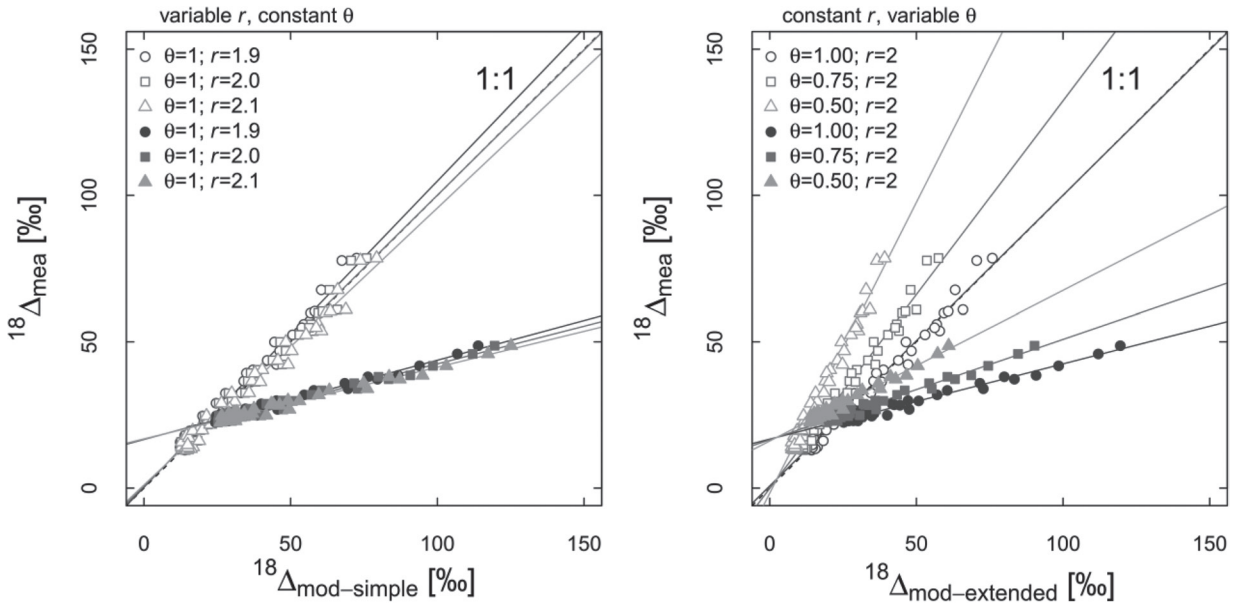

Fig. 7. Left: Relationship between simple modelled discrimination against $C^{18}OO$ ($^{18}\Delta_{mod\text{-}simple}$) versus measured discrimination against $C^{18}OO$ ($^{18}\Delta_{mea}$) in the shoot. Right: Relationship between extended modelled discrimination against $C^{18}OO$ ($^{18}\Delta_{mod\text{-}extended}$) versus measured discrimination against $C^{18}OO$ ($^{18}\Delta_{mea}$) in the shoot. Control treatment is shown by open symbols, drought treatment by closed symbols, and $x=y$ by dashed lines. θ, ^{18}O equilibrium; r, retroflux factor. Results are shown as least squares linear regressions (solid lines, all $R^2>0.97$ and $P<0.001$). Data shown are individual measurements from the label day between 11 a.m. and 7 p.m.

can be dismissed (Affek *et al.*, 2006; Griffis *et al.*, 2011). It should be noted that the ^{18}O equilibrium presented here is rather an apparent equilibrium, which also summarizes effects that result from measuring an entire shoot. Thus, the measurements include effects from stem respiration, shading, etc., which are not present when measuring single leaves as done in most other laboratory studies.

In a model approach, Xiao *et al.* (2010) pointed out the need for a better understanding of environmental controls on CO_2 hydration efficiency, as they concluded that only θ=0.46 was able to logically explain the disagreement between simulated and observed ^{18}O isoforcing for a soybean field. Low θ values have been confirmed during other field measurements in C_3 ecosystems (*F. sylvatica*) with a chamber approach (θ=0.7; A. Hammerle, L. Gentsch, P. Sturm, M. Barthel, R. Siegwolf, N. Buchmann, and A. Knohl, unpublished data). Using eddy covariance measurements, Griffis *et al.* (2011) further showed for a C_4 ecosystem that θ can markedly differ when estimating θ for the canopy scale (θ=0.2) compared with the leaf scale (θ=0.7).

Overall, we showed that $H_2{}^{18}O$ labelling in combination with laser spectroscopy can be used to investigate the speed of the link between below- and aboveground processes under drought conditions by measuring the $^{18}O/^{16}O$ ratio in CO_2 and H_2O_v. We conclude that drought impairs the ^{18}O signal propagation from below- to aboveground and reduces the ^{18}O equilibrium between CO_2 and H_2O at the shoot level. An instantaneous ^{18}O exchange as observed in the shoot was not present in the soil. To summarize, drought stress affects $C^{18}OO$ fluxes within the soil–plant–atmosphere system at different temporal and spatial scales, highlighting complex interactions between different components. Despite the existing published research body, there is need for further experimental work to constrain model approaches such as those of Riley *et al.* (2002, 2003). With the fast development of optical measurement techniques for isotope research (reviewed by Griffis, 2013), there is a promising basis for extended research in this area.

Supplementary data

Supplementary data are available at *JXB* online.

Supplementary information. Potential error estimation on δ value from condensation.

Acknowledgements

The authors thank P. Plüss, P. Flütsch, and T. Baur for their outstanding technical support and help concerning the measurement set-up. The authors also acknowledge R.A. Werner for liquid water laser measurements, A. Ackermann for IRMS measurements at the Isolab of the Grassland Sciences Group at ETH Zurich, and four anonymous reviewers improving the overall quality of the manuscript. This work was supported by a 'Marie Curie Excellence Grant' granted by the European Commission to AK (MEXT-CT-2006–042268) and by a start-up grant from ETH Zurich to AK. The Crown Research Institute (CRI) Landcare Research is acknowledged for salary for MB to finalize this manuscript.

References

Affek HP, Krisch MJ, Yakir D. 2006. Effects of intraleaf variations in carbonic anhydrase activity and gas-exchange on leaf $C^{18}OO$ isoflux in *Zea mays*. *New Phytologist* **169,** 321–329.

Barthel M, Hammerle A, Sturm P, Gentsch L, Baur T, Knohl A. 2011*a*. The diel imprint of leaf metabolism on the $\delta^{13}C$ signal of soil respiration under control and drought conditions. *New Phytologist* **192,** 925–938.

Barthel M, Sturm P, Knohl A. 2011*b*. Soil matrix contamination and canopy recycling did not impair $^{13}CO_2$ plant-soil pulse labeling experiments. *Isotopes in Environment and Health Studies* **47,** 1–13.

Bowling DR, McDowell NG, Welker JM, Bond BJ, Law BE, Ehleringer JR. 2003. Oxygen isotope content of CO_2 in nocturnal ecosystem respiration: 2. Short-term dynamics of foliar and soil component fluxes in an old-growth ponderosa pine forest. *Global Biochemical Cycles* **17,** 1124.

Brenninkmeijer CAM, Kraft P, Mook WG. 1983. Oxygen isotope fractionation between CO_2 and H_2O. *Isotope Geoscience* **1,** 181–190.

Buck AL. 1981. New equations for computing vapor-pressure and enhancement factor. *Journal of Applied Meteorology* **20,** 1527–1532.

Cermak J, Matyssek R, Kucera J. 1993. Rapid response of large, drought-stressed beech trees to irrigation. *Tree Physiology* **12,** 281–290.

Cernusak LA, Farquhar GD, Wong SC, Stuart-Williams H. 2004. Measurement and interpretation of the oxygen isotope composition of carbon dioxide respired by leaves in the dark. *Plant Physiology* **136,** 3350–3363.

Cernusak LA, Kahmen A. 2013. The multifaceted relationship between leaf water ^{18}O enrichment and transpiration rate. *Plant, Cell & Environment* **36,** 1239–1241.

Ciais P, Denning AS, Tans PP, *et al.* 1997. A three-dimensional synthesis study of $\delta^{18}O$ in atmospheric CO_2 1. surface fluxes. *Journal of Geophysical Research* **102,** 5857–5872.

Cousins AB, Badger MR, von Caemmerer S. 2006. A transgenic approach to understanding the influence of carbonic anhydrase on $C^{18}OO$ discrimination during C_4 photosynthesis. *Plant Physiology* **142,** 662–672.

Craig H, Gordon LI. 1965. *Deuterium and ^{18}O variations in the ocean and marine atmosphere*. Pisa, Italy: Consiglio Nationale Delle Ricerche Laboratorio Di Geologia Nucleare.

Edwards EJ, Still CJ, Donoghue J. 2007. The relevance of phylogeny to studies of global change. *Trends in Ecology and Evolution* **22,** 243–249.

Evans JR, Sharkey TD, Berry JA, Farquhar GD. 1986. Carbon isotope discrimination measuered concurrently with gas exchange to investigate CO_2 diffusion in leaves of higher plants. *Australian Journal for Plant Physiology* **13,** 281–292.

Farquhar G, Lloyd J. 1993. Carbon and oxygen isotope effects in the exchange of carbon dioxide between terrestrial plants and the atmosphere. In: Ehleringer JR, Hall AE, Farquhar G, eds. *Stable isotopes and plant carbon–water relations*., San Diego, CA: Academic Press, 47–70.

Farquhar GD, Lloyd J, Taylor JA, Flanagan LB, Syvertsen JP, Hubick KT, Wong SC, Ehleringer JR. 1993. Vegetation effects on the isotope composition of oxygen in atmospheric CO_2. *Nature* **363,** 439–442.

Francey RJ, Tans PP. 1987. Latitudinal variation in oxygen-18 of atmospheric CO_2. *Nature* **327,** 495–497.

Gartner K, Nadezhdina N, Englisch M, Cermack J, Leitgeb E. 2009. Sap flow of birch and Norway spruce during the European heat and drought in summer 2003. *Forest Ecology and Management* **258,** 590–599.

Gillon J, Yakir D. 2000*a*. Naturally low carbonic anhydrase activity in C_4 and C_3 plants limits discrimination against $C^{18}OO$ during photosynthesis. *Plant, Cell & Environment* **23,** 903–915.

Gillon J, Yakir D. 2000*b*. Internal conductance to CO_2 diffusion and $C^{18}OO$ discrimination in C_3 leaves. *Plant Physiology* **123,** 201–213.

Gillon J, Yakir D. 2001. Influence of carbonic anhydrase activity in terrestrial vegetation on the ^{18}O content of atmospheric CO_2. *Science* **291,** 2584–2587.

Gollan T, Passioura JB, Munns R. 1986. Soil water status affects the stomatal conductance of fully turgid wheat and sunflower leaves. *Australian Journal of Plant Physiology* **13,** 459–464.

Gonfiantini R, Gratziu S, Tongiorgi E 1965. Oxygen isotope composition of water in leaves. In *Isotopes and radiation in soil–plant nutrition studies*. Vienna, Austria: International Atomic Energy Agency, 405–410.

Granier A, Reichstein M, Breda N, *et al*. 2007. Evidence for soil water control on carbon and water dynamics in European forests during the extremely dry year: 2003. *Agricultural and Forest Meteorology* **143,** 123–145.

Griffis TJ. 2013. Tracing the flow of carbon dioxide and water vapor between the biosphere and atmosphere: A review of optical isotope techniques and their application. *Agricultural and Forest Meteorology* **174–175,** 85–109.

Griffis TJ, Lee X, Baker JM, Billmark K, Schultz N, Erickson M, Zhang X, Fassbinder J, Xiao W, Hu N. 2011. Oxygen isotope composition of evapotranspiration and its relation to C_4 photosynthetic discrimination. *Journal of Geophysical Research-Biogeosciences* **116,** 1–21.

Guliyev N, Bayramov S, Babayev H. 2008. Effect of water deficit on RUBISCO and carbonic anhydrase activities in different wheat genotypes. *Photosynthesis. Energy from the Sun: 14th International Congress on Photosynthesis* **91,** 1465–1468.

Harwood KG, Gillon JS, Griffiths H, Broadmeadow MSJ. 1998. Diurnal variation of $\Delta^{13}CO_2$, $\Delta C^{18}O^{16}O$ and evaporative site enrichment of $\delta H_2{}^{18}O$ in *Piper aduncum* under field conditions in Trinidad. *Plant, Cell & Environment* **21,** 269–283.

Horita J, Wesolowski DJ. 1994, Liquid-vapor fractionation of oxygen and hydrogen isotopes of water from the freezing to the critical temperature. *Geochimica et Cosmochimica Acta* **58,** 3425–3437.

Kato T, Nakazawa T, Aoki S. 2004. Seasonal variation of the oxygen isotopic ratio of atmospheric carbon dioxide in a temperate forest, Japan. *Global Biochemical Cycles* **18,** GB2020.

Kayler Z, Gessler A, Buchmann N. 2010. What is the speed of link between aboveground and belowground processes? *New Phytologist* **187,** 886–888.

Kesselmeier J, Hubert A. 2002. Exchange of reduced volatile sulfur compounds between leaf litter and the atmosphere. *Atmospheric Environment* **36,** 4679–4686.

Kesselmeier J, Teusch N, Kuhn U. 1999. Controlling variables for the uptake of atmospheric carbonyl sulfide by soil. *Journal of Geophysical Research* **104,** 11577–11584.

Kirschbaum MUF. 1988. Recovery of photosynthesis from water stress in *Eucalyptus pauciflora*—a process in two stages. *Plant, Cell & Environment* **11,** 685–694.

Luz B, Barkan E, Yam R, Shemesh A. 2009. Fractionation of oxygen and hydrogen isotopes in evaporating water. *Geochimica et Cosmochimica Acta* **73,** 6697–6703.

Merlivat L. 1978. Molecular diffusitivities of $H_2{}^{18}O$ in gases. *Journal of Chemical Physics* **69,** 2864–2871.

Miller JB, Yakir D, White JWC, Tans PP. 1999. Measurement of $^{18}O/^{16}O$ in the soil-atmosphere CO_2 flux. *Global Biochemical Cycles* **13,** 761–774.

Mills GA, Urey HC. 1940. The kinetics of isotopic exchange between carbon dioxide, bicarbonate ion, carbonate ion and water. *Journal of the American Chemical Society* **62,** 1019–1026.

Nadezhdina N. 1999. Sap flow index as an indicator of plant water status. *Tree Physiology* **19,** 885–891.

Nelson DD, McManus JB, Herndon SC, Zahniser MS, Tuzson B, Emmenegger L. 2008. New method for isotopic ratio measurements of atmospheric carbon dioxide using a 4.3 μm pulsed quantum cascade laser. *Applied Physics B—Lasers and Optics* **90,** 301–309.

R Development Core Team. 2011. R: A language and environment for statistical computing. R Foundation for Statistical Computing, Vienna, Austria. http://www.r-project.org.

Riley WJ. 2005. A modeling study of the impact of the $\delta^{18}O$ value of near-surface soil water on the $\delta^{18}O$ value of the soil-surface CO_2 flux. *Geochimica et Cosmochimica Acta* **69,** 1939–1946.

Riley WJ, Still CJ, Helliker BR, Ribas-Carbo M, Berry JA. 2003. ^{18}O composition of CO_2 and H_2O ecosystem pools and fluxes in a tallgrass prairie: simulations and comparisons to measurements. *Global Change Biology* **9,** 1567–1581.

Riley WJ, Still CJ, Torn MS, Berry JA. 2002. A mechanistic model of $H_2{}^{18}O$ and $C^{18}OO$ fluxes between ecosystems and the atmosphere: model description and sensitivity analyses. *Global Biochemical Cycles* **16,** 1095.

Rühr NK, Offermann CA, Gessler A, Winkler JB, Ferrio JP, Buchmann N, Barnard RL. 2009. Drought effects on allocation of recent carbon: from beech leaves to soil CO_2 efflux. *New Phytologist* **184**(4): 950–961.

Schär C, Vidale PL, Lüthi D, Frei C, Häberli C, Liniger MA, Appenzeller C. 2004. The role of increasing temperature variability in European summer heatwaves. *Nature* **427,** 332–335.

Seibt U, Wingate L, Lloyd J, Berry JA. 2006. Diurnally variable $\delta^{18}O$ signatures of soil CO_2 fluxes indicate carbonic anhydrase activity in forest soil. *Journal of Geophysical Research* **111,** G04005.

Silverman DN. 1982. Carbonic anhydrase: ^{18}O-exchange catalyzed by an enzyme with rate contributing proton-transfer steps. *Methods in Enzymology* **87,** 732–752.

Skirrow G. 1975. The dissolved gases-carbon dioxide. In Riley JP, Skirrow G, eds. *Chemical oceanography*. San Diego, CA: Academic Press, 1–92.

Stern L, Baisden WT, Amundson R. 1999. Processes controlling the oxygen isotope ratio of soil CO_2, Analytic and numerical modeling. *Geochimica et Cosmochimica Acta* **63,** 799–814.

Stern LA, Amundson R, Baisden WT. 2001. Influence of soils on oxygen isotope ratio of atmospheric CO_2. *Global Biochemical Cycles* **15,** 753–759.

Stöhr A, Lösch R. 2004. Xylem sap flow and drought stress of *Fraxinus excelsior* saplings. *Tree Physiology* **24,** 169–180.

Sturm P, Eugster W, Knohl A. 2012. Eddy covariance measurements of CO_2 isotopologues with a quantum cascade absorption spectrometer. *Agricultural and Forest Meteorology* **152,** 73–82.

Sturm P, Knohl A. 2010. Water vapor δ^2H and $\delta^{18}O$ measurements using off-axis integrated cavity output spectroscopy. *Atmospheric Measurement Techniques* **3,** 67–77.

Tans PP. 1998. Oxygen isotopic equilibrium between carbon dioxide and water in soils. *Tellus* **50B**: 163–178.

von Caemmerer S and Farquhar GD. 1981. Some relationships between the biochemistry of photosynthesis and the gas-exchange of leaves. *Planta* **153,** 376–387.

Wingate L, Seibt U, Maseyk K, Ogee, J, Almeida P, Yakir D, Pereira JS. 2008. Evaporation and carbonic anhydrase activity recorded in oxygen isotope signatures of net CO_2 fluxes from a Mediterranean soil. *Global Change Biology* **14,** 2178–2193.

Xiao W, Lee X, Griffis TJ, Kim K, Welp LR, Yu Q. 2010. A modeling investigation of canopy-air oxygen isotopic exchange of water vapor and carbon dioxide in a soybean field. *Journal of Geophysical Research* **115,** G01004.

Yakir D. 2003. The stable isotopic composition of atmospheric CO_2. In: Keeling RF, ed. *Treatise on Geochemistry, Vol. 4. The Atmosphere*. Oxford: Elsevier, 175–205.

Yakir D, Sternberg LSL 2000. The use of stable isotopes to study ecosystem gas-exchange. *Oecologia* **123,** 297–311.

Yakir D, Wang XF. 1996. Fluxes of CO_2 and water between terrestrial vegetation and the atmosphere estimated from isotope measurements. *Nature* **380,** 515–517.